JOURNAL OF PETROLOGY | VOLUME 39 | NUMBER 11 & 12 | PAGES 1917–1930 | 1998

Carbonatite Metasomatism in the Southeastern Australian Lithosphere

GREGORY M. YAXLEY[1,*], DAVID H. GREEN[1] AND VADIM KAMENETSKY[2]

[1]RESEARCH SCHOOL OF EARTH SCIENCES, THE AUSTRALIAN NATIONAL UNIVERSITY, CANBERRA, A.C.T. 0200, AUSTRALIA

[2]SRC FOR ORE DEPOSIT RESEARCH, UNIVERSITY OF TASMANIA, GPO BOX 252-79, HOBART, TAS. 7001, AUSTRALIA

RECEIVED SEPTEMBER 30, 1997; REVISED TYPESCRIPT ACCEPTED MAY 21, 1998

New mineralogical and geochemical data from a suite of glass ± apatite ± amphibole ± phlogopite ± carbonate-bearing spinel wehrlite, lherzolite and harzburgite xenoliths from the Newer Volcanics, southeastern Australia, are consistent with metasomatic interactions between harzburgitic or refractory lherzolitic lithosphere, and penetrative sodic dolomitic carbonatite melts. Metasomatism occurred when ascending dolomitic carbonatites crossed the reaction enstatite + dolomite = forsterite + diopside + CO_2 at ~1·5–2·0 GPa, resulting in partial to complete replacement of primary orthopyroxene by sodic clinopyroxene, together with crystallization of apatite, amphibole and phlogopite, and release of CO_2-rich fluid. In the sample suite examined, the minimum amount of carbonatite melt may be estimated on the assumption that metasomatism occurred in a closed system, and that the precursor lithology was clinopyroxene-poor harzburgite. The derivative wehrlite compositions require 6–12% carbonatite addition, the lherzolites require ~8% or less, and the harzburgites require minimal addition of carbonatite. However, metasomatism probably also involved an open system component, during which residual and metasomatic phase compositions were determined by partitioning relationships with the reacting carbonatite, resulting in loss from the metasomatized volume of a fugitive, siliceous, aluminous, alkali- and LILE-enriched silicate melt.

KEY WORDS: *carbonatite*; *metasomatism*; *peridotite*; *xenolith*; *lithosphere*

INTRODUCTION

It has long been established from isotopic studies that crustally emplaced carbonatites were ultimately derived from the mantle (Deines & Gold, 1973; Nelson *et al.*, 1988). However, controversy remains as to whether such magmas represent (1) direct partial melts of carbonate-bearing mantle peridotite (i.e. primary carbonatites; Wyllie & Huang, 1975; Wallace & Green, 1988; Sweeney, 1994), (2) primary carbonatites modified by interactions with peridotite wall-rock in the upper mantle (Wallace & Green, 1988; Dalton & Wood, 1993; Sweeney *et al.*, 1994), or (3) highly evolved products of crystal fractionation (Lee & Wyllie, 1997) or silicate–carbonate liquid immiscibility (Kjarsgaard & Hamilton, 1988, 1989; Lee & Wyllie, 1997) from mantle-derived carbonated undersaturated silicate melts.

Central to this debate is the existence or otherwise of carbonate-rich melts in the upper mantle. Several high-pressure experimental studies have shown that carbonate melts can exist in equilibrium with peridotite over a range of upper-mantle conditions of pressure, temperature, bulk composition and volatile content (Wyllie & Huang, 1975; Wallace & Green, 1988; Thibault *et al.*, 1992; Dalton & Wood, 1993; Sweeney, 1994; Sweeney *et al.*, 1994). In addition, a number of studies of mantle-derived spinel peridotite xenoliths have attributed petrographic features such as evidence of reaction of primary phases with carbonate, unusually high ratios of clinopyroxene to orthopyroxene, and/or the presence of apatite, amphibole or carbonate, to interaction of refractory lithosphere with invasive carbonatite melts at pressures of ~1·5–2 GPa. This process produces moderate to extreme large ion lithophile element (LILE) enrichment, which is decoupled from Ti abundances (Green & Wallace, 1988; Yaxley *et al.*, 1991; Dautria *et al.*, 1992; Rudnick *et al.*,

*Corresponding author. Telephone: +61.2.6249.3350. Fax: +61.2.6249.5989. e-mail: Greg.Yaxley@anu.edu.au

1992, 1993; Hauri *et al.*, 1993; Ionov *et al.*, 1993, 1996; Chazot *et al.*, 1996).

In this contribution we use new petrographic, mineralogical and geochemical data from 32 spinel peridotite xenoliths hosted by the Newer Volcanics (southeastern Australia; SEA), to further support experimentally based conclusions that carbonate melts can exist within the upper mantle, and to increase understanding of their role in its metasomatic enrichment. Part of this suite was described by Yaxley *et al.* (1991), and includes samples from Mt Leura and Mt Shadwell. We describe additional samples from these localities, as well as from Mt Noorat, Lake Bullenmerri and The Anakies. New samples were selected on the basis that they also exhibit modal evidence of carbonatite metasomatism.

ANALYTICAL TECHNIQUES

Mineral phases were analysed using a Cameca SX50 electron microprobe at the University of Tasmania. The instrument was calibrated using recognized international natural mineral standards, and PAP data reduction was employed. Carbonates and glasses were analysed using an accelerating voltage of 15 kV and a beam current of 10 nA. A broad beam was used to minimize sample damage and potential loss of volatile elements such as Na. Other phases (silicates, apatite and spinel) were analysed with an accelerating voltage of 15 kV and beam current of 20 nA, using a focused, 1 μm diameter beam.

Whole-rock major and minor elements, and some trace elements (Ba [3], Sc [1], Nb [1], Zr [1], Y [1·5], Sr [2], Rb [2], Cr [2], Ni [1] and V [3]; detection limits in ppm are in brackets) were determined using a Phillips PW 1410 X-ray fluorescence spectrometer at the University of Tasmania. Other trace elements were determined by instrumental neutron activation analysis at Becquerel Laboratories, Lucas Heights, N.S.W. Elements analysed include La [0·1], Ce [1·0], Nd [2·0], Sm [0·05], Eu [0·2], Tb [0·5], Ho [0·5], Yb [0·1], Lu [0·1], Sc [0·05], Hf [0·1], Ta [0·2] and Th [0·2].

PETROGRAPHY AND MINERAL CHEMISTRY

Coarse-grained phases

Our samples are spinel wehrlites, lherzolites and harzburgites, in which large porphyroblastic grains of olivine, and clinopyroxene ± orthopyroxene occur within a finer matrix of well-annealed olivine and clinopyroxene (± minor orthopyroxene) neoblasts. Olivine compositions are similar to those from peridotites from other localities, with forsterite (Fo) from 86·0 to 91·6 mol %, and NiO from 0·27 to 0·43 wt %. CaO contents (≤0·06 wt %) are also typical of mantle olivine. Orthopyroxene grains, however, have slightly higher SiO_2, and distinctly lower Al_2O_3 contents in comparison with orthopyroxene from other peridotite xenoliths (Fig. 1a; Table 1). Clinopyroxene porphyroclasts and neoblasts are Cr-diopside rich, and in this respect are similar to clinopyroxenes from other peridotite suites. However, they have lower Al_2O_3 and TiO_2, and higher Cr_2O_3, Na_2O and SiO_2 than many clinopyroxenes from other spinel peridotites (Fig. 1b–d; Table 1).

All samples contain large vesicular patches of siliceous, aluminous and alkali-rich glass containing secondary microlites of olivine, clinopyroxene and spinel (Yaxley *et al.*, 1997). The glassy patches are usually in contact with, and have clearly partially replaced porphyroclastic or neoblastic clinopyroxene and/or orthopyroxene. Grains of embayed, rounded primary Cr-rich spinel frequently occur within the cores of the glassy patches. The spinels extend to unusually high *cr*-numbers [where *cr*-number = $100Cr/(Cr + Al + Fe^{3+})$], ranging from 25 to 85, with most >70. In general, primary spinels from the wehrlites have the highest *cr*-numbers, followed by the lherzolites and harzburgites. The *mg*-numbers [where *mg*-number = $100Mg/(Mg + Fe^{2+})$] are lower than, and TiO_2 contents are similar to, those of spinels reported from many other xenoliths (35–75 and 0·03–0·9 wt %, respectively).

In six samples, the spinel grains are associated with embayed, coarse-grained pargasitic amphibole or phlogopite, which has clearly partially melted to produce the surrounding glass. Amphibole and phlogopite from these samples are compositionally similar to these phases in samples from other suites (e.g. Canil & Scarfe, 1989; O'Reilly *et al.*, 1991). Amphiboles are pargasitic, with *mg*-number* [where *mg*-number* = $100Mg/(Mg + \Sigma Fe)$] from 87·2 to 91·1, 0·7–3·3 wt % TiO_2, 3·2–3·7 wt % Na_2O and ~1 wt % K_2O. Phlogopites contain 7–9 wt % K_2O and up to 1·6 wt % Na_2O. The glassy patches and associated phases have been described in detail by Yaxley *et al.* (1991, 1997).

In most samples, up to 2 modal % apatite is patchily distributed along grain boundaries, interstitial to coarse-grained primary olivine. It displays an anhedral habit, and is usually cloudy in appearance, because of abundant tiny CO_2-rich fluid inclusions.

Mineral, glass and fluid inclusions in coarse-grained clinopyroxene and other phases

A notable feature of the coarse clinopyroxene grains is the abundance of mineral and glass-bearing inclusions that they host. For example, in some samples (e.g. SH19, 76987, 71004, SH35, 76988, 71001, 71000) olivine (± Cr-rich spinel) occurs as large, rounded inclusions (up to

Table 1: Representative electron microprobe analyses of phases from some samples in the current suite

	Orthopyroxene					Metasomatic clinopyroxene				
Sample:	71007	71004	76993	76995	70982	76987	71001	2631	71004	76988
Locality:	Mt Leura	Mt Leura	Mt Shadwell	Mt Shadwell	Mt Leura	The Anakies	Mt Leura	Mt Leura		
Mineralogy:	ApAmPhGlSpWeh	ApAmPhGlSpLhz	CbApGlSpWeh	CbApGlSpHz	ApSpHz	ApGlWeh	ApGlSpWeh	ApGlSpWeh	ApAmPhGlSpLhz	ApGlSpWeh
SiO_2	57·71	56·20	57·47	57·00	57·48	53·94	54·73	54·18	53·38	54·01
TiO_2	0·01	0·01	0·02	0·03	0·02	0·02	0·34	0·03	0·56	0·08
Al_2O_3	1·32	2·54	0·87	1·42	1·19	1·87	1·65	1·90	4·07	3·27
Cr_2O_3	0·29	0·04	0·30	0·36	0·35	0·74	3·48	1·69	1·67	1·43
FeO	6·20	5·97	5·71	5·63	5·54	2·78	2·36	2·23	2·31	2·09
MnO	0·19	0·21	0·14	0·13	0·17	0·11		0·10	0·07	0·04
MgO	34·73	34·04	34·65	34·81	34·92	16·12	15·62	15·94	15·86	16·01
CaO	0·40	0·44	0·43	0·49	0·48	22·16	19·94	21·30	19·77	21·31
Na_2O	0·08	0·08	0·09	0·09	0·13	1·37	2·05	1·74	1·93	1·53
Total	100·93	99·53	99·68	99·96	100·28	99·11	100·17	99·11	99·62	99·77
mg-no.*	90·89	91·04	91·54	91·68	91·82	91·18	92·18	92·72	92·44	93·17

'Orthopyroxene' and 'Metasomatic clinopyroxene' refer to coarse-grained porphyroclastic or neoblastic grains. Locality is indicated for each sample. The row entitled 'Mineralogy' gives the mineral assemblage present in each sample. Abbreviations: Ap, apatite interstitial to primary phases and glassy patches; Cb, carbonate inclusions in clinopyroxene or glassy patches; Gl, glass patches and veins interstitial to primary phases; Am, coarse-grained amphibole; Ph, coarse-grained phlogopite; Sp, primary spinel; Weh, wehrlite; Lhz, lherzolite; Hz, harzburgite. *mg*-number* = [100Mg/(Mg + Fe)].

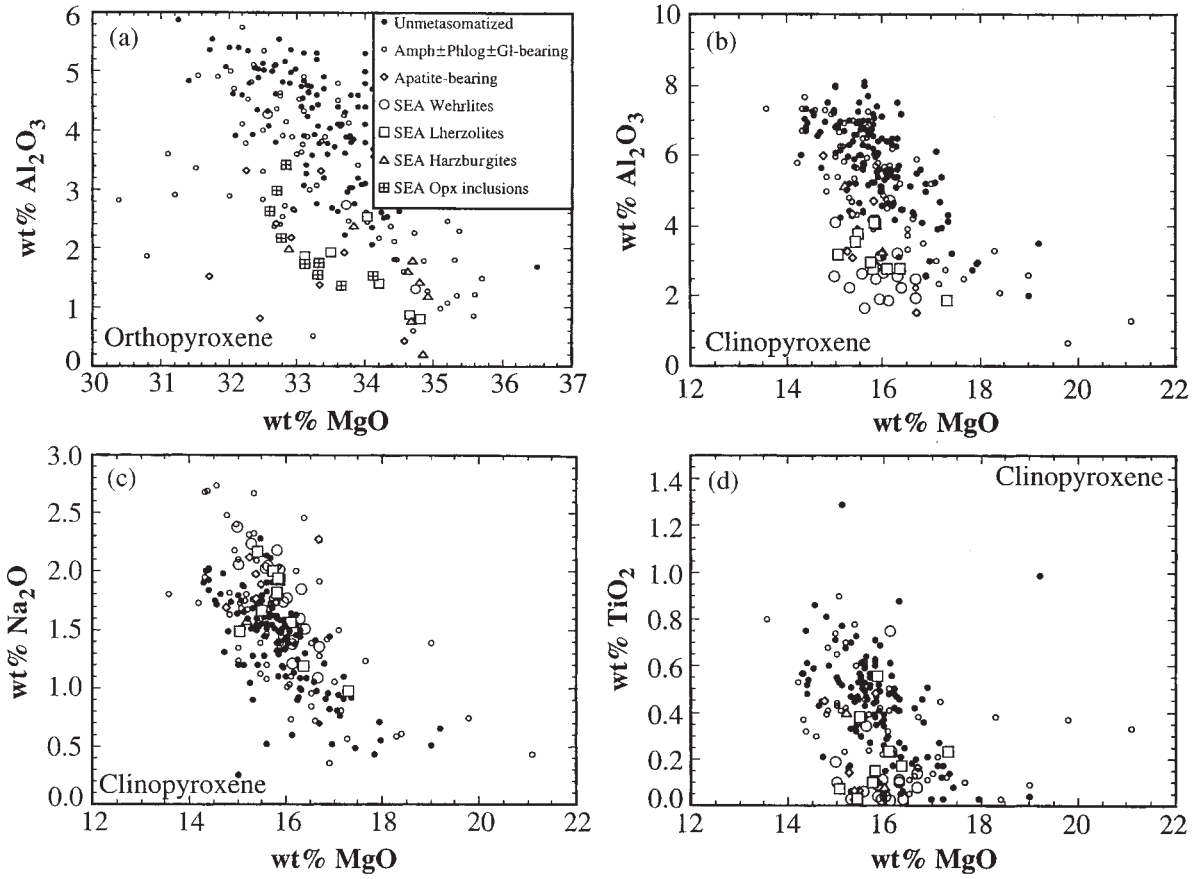

Fig. 1. Plots of oxides vs wt % MgO comparing pyroxene compositions from the SEA suite of metasomatized wehrlites, lherzolites and harzburgites with pyroxenes from anhydrous, amphibole ± phlogopite ± glass-bearing, and apatite-bearing spinel peridotite xenoliths from localities around the world. (a) wt % MgO vs wt % Al_2O_3 for primary orthopyroxenes, and for orthopyroxenes included in coarse-grained clinopyroxenes in the SEA suite, (b) wt % Al_2O_3 vs wt % MgO for clinopyroxenes, (c) wt % Na_2O vs wt % MgO for clinopyroxenes, and (d) wt % TiO_2 vs wt % MgO for clinopyroxenes. It should be noted that the current suite has orthopyroxenes and clinopyroxenes that are low in Al_2O_3, and clinopyroxenes that are low in TiO_2, but high in Na_2O, compared with anhydrous and amphibole ± phlogopite ± glass-bearing examples; also, pyroxenes from many apatite-bearing samples from other suites are compositionally similar to those from the current suite. Data sources available from the authors.

~150 μm) within coarse clinopyroxene grains. These olivine inclusions are richer in CaO (up to 0·24 wt %), and may have 1–2 mol % more Fo than coexisting primary olivine. In some wehrlites and lherzolites, large (up to ~500 μm) irregularly shaped grains of orthopyroxene are included in coarse, porphyroclastic clinopyroxene (Fig. 2a). Adjacent orthopyroxene inclusions exhibit simultaneous extinction, indicating replacement of a former larger orthopyroxene grain by clinopyroxene. The orthopyroxene inclusions have similar compositions to coexisting coarse-grained orthopyroxene grains (Fig. 1a; Table 2). Apatite also occurs frequently as small inclusions in clinopyroxene (10–20 μm across; Fig. 2b), sometimes associated with siliceous, aluminous, alkali- and P_2O_5-rich glass. Clinopyroxenes from many samples also contain lenticular, or irregularly shaped amphibole and/or phlogopite inclusions (up to 100 μm) (Fig. 2c). Amphibole found as inclusions in coarse clinopyroxene grains is similar in composition to the coarse-grained variety, although somewhat lower in TiO_2 (Table 2).

Glass is also present as inclusions in coarse clinopyroxene grains in most samples. Often the glass-bearing inclusions in clinopyroxenes contain only glass (e.g. SH64, 76996, and SH5) (Fig. 2d), but sometimes glass is present with one or more phase, including amphibole, phlogopite, olivine, apatite, orthopyroxene, spinel, Fe-sulphide or carbonate. Glass associated with phases included in clinopyroxene is siliceous, aluminous and alkali rich (Table 2). Primary olivines from some samples host very rare, rounded inclusions, 10–30 μm across, which contain glass + vapour ± daughter phase(s).

Table 2: Representative compositions of phases and glass found as inclusions hosted by coarse-grained clinopyroxene

	Amph	Amph	Phlog	Phlog	Opx	Olivine	Olivine	Carb	Glass	Glass
Sample:	70987	71004	70987	SH45	SH45	71000	71001	SH45	76991	71004
Locality:	Mt Leura	Mt Leura	Mt Leura	Mt Shadwell	Mt Shadwell	Mt Leura	Mt Leura	Mt Shadwell	Mt Leura	Mt Leura
Mineralogy:	ApGlSpLhz	ApAmPhGlSpLhz	ApGlSpLhz	CbGlSpWeh	CbGlSpWeh	ApAmGlSpWeh	ApGlSpWeh	CbGlSpWeh	ApGlSpWeh	ApAmPhGlSpLhz
SiO_2	44·71	46·00	38·69	39·03	56·52	42·40	40·60	0·21	59·51	51·12
TiO_2	1·30	1·59	1·35	1·12	0·00	0·00	0·00	0·09	0·37	0·54
Al_2O_3	12·32	11·76	16·57	15·65	1·76	0·00	0·00	0·16	19·92	22·01
Cr_2O_3	2·48	2·19	1·53	0·27	0·50	0·01	0·00	0·04	0·01	0·11
FeO	3·23	3·26	4·11	3·67	6·07	6·94	10·42	0·06	2·71	4·81
MnO	0·00	0·17	0·05	0·03	0·23	0·29	0·03	0·22	0·10	0·07
MgO	17·53	18·56	22·07	23·04	33·33	51·75	47·46	4·71	2·07	1·37
CaO	10·50	10·94	0·00	0·71	0·70	0·24	0·13	47·40	2·05	0·50
Na_2O	3·14	3·44	0·66	1·16	0·00	0·00	0·00	0·00	9·36	13·72
K_2O	0·89	0·71	8·61	7·60	0·06	0·00	0·00	0·09	2·30	2·22
P_2O_5	0·23	0·22	0·08	0·09	0·11	0·00	0·00	0·33	0·30	0·30
NiO	0·00	0·37	0·00	0·19	0·00	0·47	nd	0·06	0·22	0·00
Total	96·33	99·21	93·72	92·56	99·28	102·10	98·64	53·37	98·92	96·77
mg-no.*	90·63	91·03	90·54	91·79	90·73	93·00	89·03	99·29	57·65	33·67

Symbols and abbreviations as in Table 1.

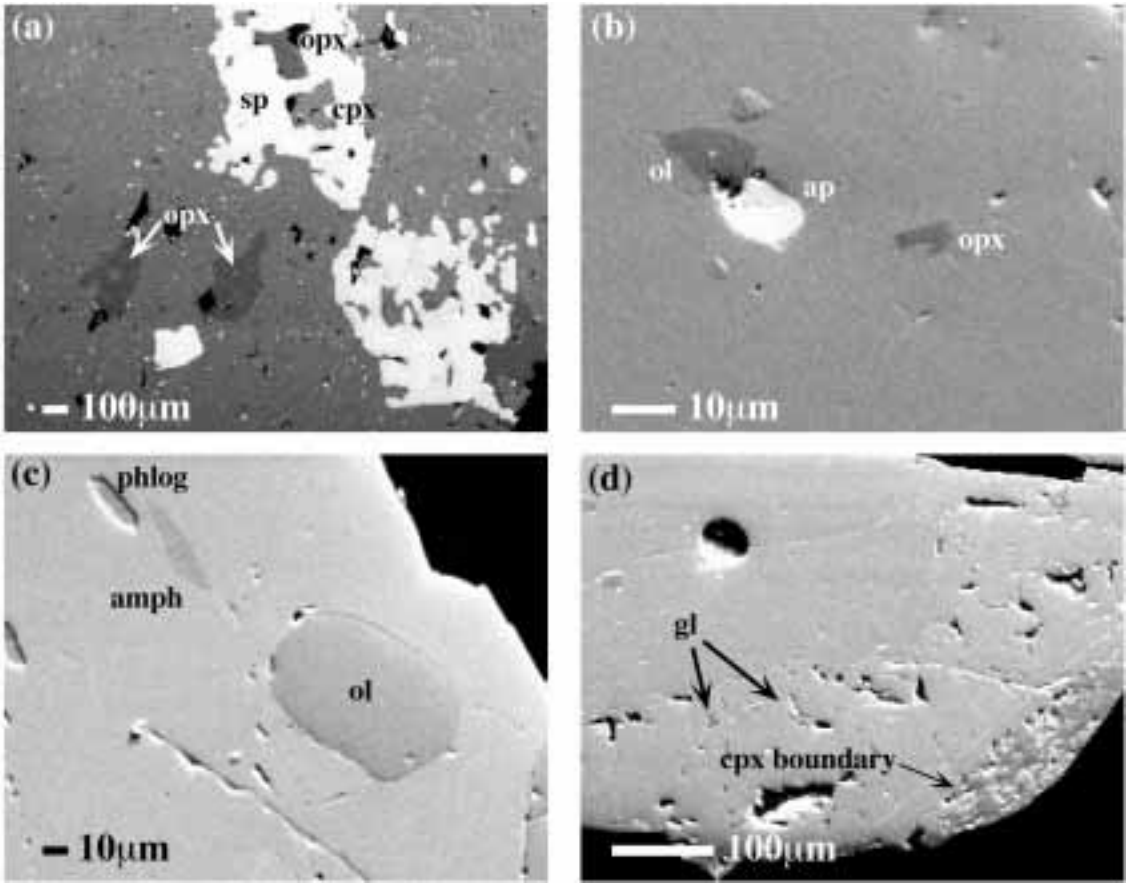

Fig. 2. Back-scattered electron images of coarse-grained clinopyroxene (cpx) and included phases from four samples. (a) Sample SH45, showing relict primary orthopyroxene (opx) grains. The two grains to the left of and below the centre are optically continuous under the petrological microscope, indicating replacement of a larger orthopyroxene grain by the host clinopyroxene. The cpx is also replacing primary spinel (sp). (b) Sample 70987, showing an olivine (ol) + apatite (ap) inclusion, and an orthopyroxene inclusion. (c) Sample 71000, showing separate inclusions of phlogopite (phlog), amphibole (amph) and olivine (ol). (d) Sample 76991 showing tiny glass patches and veinlets (gl) near the margin of a clinopyroxene grain.

Calcitic carbonate (*mg*-number 96–99; wt % MgO 2·2–4·7) occurs as rounded inclusions (20–30 μm) in coarse clinopyroxene or primary olivine, or as rounded blebs in the large, interstitial glassy patches (Yaxley *et al.*, 1997).

CO_2 is present in large (up to 50 μm) primary fluid inclusions, particularly in coarse-grained clinopyroxene and apatite, and in secondary fluid inclusions forming trails along healed fractures in other primary phases (particularly olivine and orthopyroxene). A detailed description of mineral, glass and fluid inclusions in clinopyroxene and other phases in these samples will be presented elsewhere.

Interpretation of petrography

The inclusions of olivine, orthopyroxene, amphibole, phlogopite, apatite and carbonate (± glass) (Fig. 2), which are hosted by coarse-grained clinopyroxene, are inferred either to have been trapped during crystallization of the host grain, or to represent relicts after replacement of the inclusion phase(s) by the host clinopyroxene. Except for olivine and orthopyroxene, the phases present in the inclusions match the coarser-grained metasomatic assemblages interstitial to primary olivine, orthopyroxene and spinel (i.e. glass ± amphibole ± phlogopite ± apatite ± carbonate), as described by Yaxley *et al.* (1991, 1997); thus our preferred interpretation is that these inclusions crystallized simultaneously with their intergranular counterparts and with the host clinopyroxene. On the other hand, unequivocal textural evidence of replacement of earlier orthopyroxene by coarse-grained clinopyroxene is preserved in some samples (Fig. 2a). This, coupled with the extreme modal clinopyroxene/orthopyroxene ratios in the wehrlites indicates that the coarse-grained clinopyroxene replaced pre-existing,

primary orthopyroxene, during the metasomatic event(s) affecting these samples.

We therefore infer that olivine, orthopyroxene, spinel and probably some clinopyroxene pre-date metasomatic alteration that led to growth of the coarse-grained clinopyroxene, and the apatite, amphibole, phlogopite and carbonate. Glass in large interstitial patches and veins, and in glass-only inclusions in clinopyroxene, post-dates metasomatism, and is probably related to partial or complete melting of the metasomatically introduced assemblage as a result of thermal and decompression effects associated with transport of the xenoliths to the surface (Yaxley *et al.*, 1997).

WHOLE-ROCK GEOCHEMISTRY

We present whole-rock geochemical data from our new samples in Table 3. In the following discussion, and in Figs 3–6, we refer to the new data and to those of Yaxley *et al.* (1991).

Plots of oxide components vs wt % MgO for >300 spinel peridotites from world-wide localities yield systematic trends (positive for compatible elements, negative for incompatible elements; Fig. 3), which are generally interpreted to result from varying degrees of basaltic or picritic melt extraction from more primitive peridotite, leaving a range of relatively refractory residues (e.g. Nickel & Green, 1984; Frey *et al.*, 1985).

The major element geochemistry of many of the current samples has been substantially perturbed from these partial melting trends exhibited by the world-wide xenolith suite. Our samples define cross-trends towards high CaO, P_2O_5, K_2O and Na_2O, and low SiO_2 and Al_2O_3 (Fig. 3a and b). However, for nearly all samples, abundances of Cr_2O_3, NiO, V and TiO_2 lie within the partial melting trends, and have apparently been undisturbed by metasomatism (Fig. 3c and d). Two samples (70987 and 71004) have higher TiO_2 contents than the remainder of the suite, partly because of the presence of high-Ti pargasite (Fig. 3c).

The harzburgites contain the highest MgO contents of the entire suite. In contrast to the wehrlites and lherzolites, most of them have apparently not been perturbed from the partial melting trends. All but one plot in a tight cluster, within the trends for SiO_2, Al_2O_3, TiO_2, Na_2O and CaO (Fig. 3).

The unusual compositions of the selected suite reflect the mineralogical characteristics described earlier. For example, high modal clinopyroxene (particularly evident in the wehrlites), and the presence of accessory apatite, is linked to unusually high values of whole-rock CaO/Al_2O_3 [from 0·68 to 5·22 with average 2·62, compared with 0·95 for 'average' subcontinental lithosphere of McDonough (1990)]. Similarly, the presence of metasomatic pargasite and sodic clinopyroxene has resulted in unusually high whole-rock Na_2O/Al_2O_3 values (0·11–0·71 with average 0·43, compared with the typical value of 0·11). The presence of modal apatite has resulted in high P_2O_5 contents [up to 0·77 wt % in sample 71001; see table 2 of Yaxley *et al.* (1991)].

This suite displays substantial enrichments in Th, Zr, Nb, Sr, Y, LREE and HREE. Primitive mantle normalized 'spidergrams' for representative wehrlites, lherzolites and harzburgites (Fig. 4) indicate strong fractionations in Ba/Th, K/La, Zr/Hf and Ti/Eu from estimated primitive mantle values (Sun & McDonough, 1989).

Of particular interest are the Ti/Eu values exhibited by the suite. These elements are generally considered not to fractionate substantially during partial melting of peridotite. As a result, most mantle-derived spinel peridotites, as well as primitive basalts, have Ti/Eu values similar to primitive mantle (7740; Sun & McDonough, 1989; Fig. 5). The present samples, however, have substantially lower whole-rock Ti/Eu values (143–3000, average 830), similar to other apatite-bearing samples from southeastern Australia (Fig. 5). This distinctive decoupling of Ti and REE abundances is a feature apparently characteristic of apatite-bearing peridotites, but was also observed in extremely refractory (apatite-free) clinopyroxene-bearing dunites from Olmani, Tanzania (Rudnick *et al.*, 1993) (Fig. 5). In addition, in a suite of amphibole $\pm$ apatite-bearing spinel lherzolites from Yemen (Chazot *et al.*, 1996), all phases containing significant proportions of the whole-rock budget for both Ti and Eu (amphibole, glass and matrix clinopyroxene), have very low Ti/Eu values (<250 for clinopyroxene, 1900–3140 for glass and 209–3570 for amphibole). It is therefore likely that the (unreported) whole-rock compositions of these samples would have low Ti/Eu.

Zr and Hf are another element pair generally considered not to fractionate significantly from the primitive mantle Zr/Hf value of 36 during partial melting of peridotite. The present samples, other apatite-bearing xenoliths from southeastern Australia (O'Reilly & Griffin, 1988; Stolz & Davies, 1988), and the clinopyroxene-bearing dunites from Olmani, Tanzania (Rudnick *et al.*, 1992, 1993), exhibit fractionations to substantially higher values. Our samples have Zr/Hf from 34 to 125 (average 66).

DISCUSSION

The nature of the metasomatic agent

Replacement of primary orthopyroxene by metasomatically introduced clinopyroxene implies interaction between harzburgitic or lherzolitic precursor wall-rock

Table 3: Whole-rock geochemical analyses for representative xenoliths

Sample:	76988	73797	76989	76990	76991	76993	70961	76994	71006	71003	70982	77000	76999	76995	71023	76997
Locality:	Mt Shadwell	Bullenmerri	Mt Shadwell	Mt Shadwell	Mt Leura	Mt Shadwell	Mt Shadwell	Mt Leura	Mt Leura	Mt Leura	Mt Leura	Mt Noorat	Mt Shadwell	Mt Shadwell	Mt Leura	Mt Shadwell
Mineralogy:	ApGlSpWeh	ApGlSpWeh	ApGlSpWeh	ApGlSpWeh	ApGlSpWeh	CbApGlSpWeh	ApGlSpLhz	ApGlSpLhz	ApAmGlSpLhz	ApGlSpHz	ApSpHz	ApGlSpHz	ApGlSpHz	CbApGlSpHz	ApGlSpHz	ApGlSpHz
SiO_2	42·85	42·15	41·20	41·75	42·55	42·15	43·58	42·59	44·36	43·52	44·16	43·75	43·65	47·02	43·73	42·66
TiO_2	0·06	0·03	0·00	0·00	0·01	0·05	0·10	0·11	0·12	0·04	0·01	0·01	0·01	0·03	0·00	0·04
Al_2O_3	1·19	1·17	0·72	0·77	0·63	0·59	1·05	1·01	2·59	1·00	0·60	0·65	0·62	1·40	0·79	0·77
Fe_2O_3	10·22	8·86	9·37	10·71	10·34	9·09	10·31	10·41	11·19	10·25	8·93	9·08	8·82	8·34	8·65	8·56
MnO	0·15	0·16	0·14	0·16	0·15	0·14	0·17	0·17	0·17	0·14	0·14	0·14	0·14	0·12	0·11	0·12
MgO	42·37	43·69	43·97	43·08	44·95	44·86	42·20	42·53	38·42	44·20	45·63	45·55	45·08	41·62	45·62	45·52
CaO	3·31	2·45	3·27	2·51	2·12	2·22	1·87	2·53	2·55	0·82	0·63	0·79	1·09	0·95	0·81	1·55
Na_2O	0·50	0·79	0·51	0·44	0·32	0·33	0·68	0·38	0·55	0·11	<0·20	<0·20	<0·20	<0·20	0·00	0·25
K_2O	0·13	0·21	0·04	0·06	0·03	0·05	0·17	0·13	0·14	0·04	0·04	0·04	0·04	0·07	0·00	0·04
P_2O_5	0·30	0·25	0·64	0·38	0·00	0·15	0·11	0·13	0·05	0·05	0·06	0·06	0·12	0·02	0·04	0·14
LOI	−0·55	−0·38	−0·55	−0·60	−0·73	−0·47	−0·71	−0·58	−0·56	−0·43	−0·60	−0·11	−0·57	−0·43	−0·46	−0·47
Total	100·53	99·38	99·31	99·26	100·37	99·16	99·53	99·41	100·05	100·32	99·60	99·96	99·00	99·14	99·29	99·18
mg-no.*	89·15	90·71	90·29	88·85	89·60	90·72	89·02	89·00	87·18	89·52	91·01	90·86	91·01	90·81	91·27	91·33
La		8·16	26·80	19·30	2·43									2·28	9·20	
Ce		20·10	52·70	34·80	6·50									5·00	15·40	
Nd		11·70	20·80	14·50	4·50									2·61	6·72	
Sm		2·51	3·45	2·80	1·23									0·51	0·90	
Eu		0·74	0·94	0·77	0·42									0·15	0·26	
Tb		0·29	0·32	0·28	0·19									0·07	0·12	
Ho		0·26	0·22	0·27	0·22									0·07	0·11	
Yb		0·34	0·30	0·30	0·32									0·13	0·08	
Lu		0·04	0·04	0·04	0·04									0·02	0·01	
Rb	<2	5	<2	<2	<2	<2	4	5	4	<2	2	3	<2	<2	<2	<2
Ba	30	48	46	18	12	26	28	36	47	25	9	20	22	25	33	19
Th		0·71	2·51	2·65	<0·10									0·31	2·32	
Nb	23·4	12	12·5	12	11·6	4·8	8·6	1·9	5	<1	2·3	4·1	7·8	5	1·8	5·5
Ta		<0·20	0·51	0·60	0·38									0·32	<0·20	
Sr	99·7	121·4	266·1	192·4	69·8	86·1	69·1	184·7	101	20	36·2	62·7	73·9	32·7	75·4	47·6
Zr	28·2	26·1	12·4	37·5	24·3	30·2	31·9	4·2	20	1·1	4·5	2·2	19·4	8·8	<2	15·8
Hf		0·28	0·19	0·54	0·30									0·19	<0·10	
Y	3·9	7·5	6·4	5·4	3·2	4·4	4·2	8·9	6	<2	<2	1·9	2·5	<2	<2	2·2
Sc	8·6	8·5	7	7·8	5	7·4	7·3	8·8	13·2	9·1	6·1	6·8	6·1	8·5	6·2	7·3
Ni	2233	2272	2361	2339	2363	2671	2287	2375	2010	2516	2454	2431	2432	2108	2447	2700
Cr	2442	2959	2615	3097	1996	3183	3122	2973	2794	3351	2182	3205	2725	3845	2466	2042
V	37·5	39·5	28·8	32·7	26·8	28·6	31·7	41·3	68·3	36·1	19·5	27·9	26·7	47·1	32·3	29·9

Abbreviations and symbols as in Table 1.

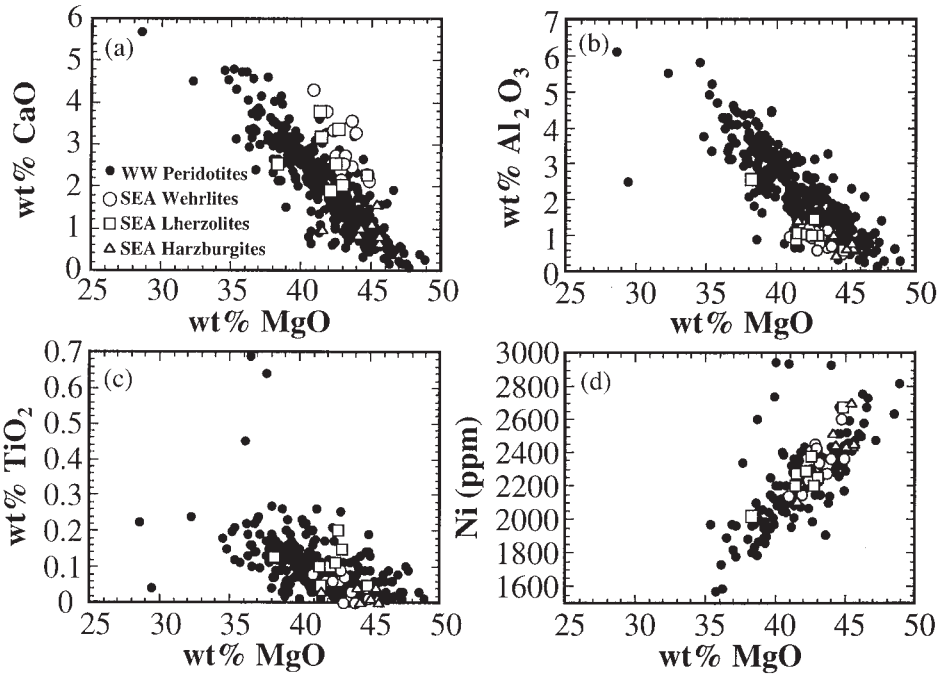

Fig. 3. Plots of (a) wt % CaO, (b) wt % Al_2O_3, (c) wt % TiO_2 and (d) Ni (ppm) against wt % MgO comparing whole-rock analyses of the current suite (SEA wehrlites, SEA lherzolites and SEA harzburgites) with published data from other xenoliths [world-wide (WW) peridotites]. The systematic variations exhibited by the world-wide suite are the result of extraction of varying amounts of picritic or basaltic melts from fertile peridotite, leaving a range of more refractory residues. Compared with these partial melting trends, the current suite has apparently been enriched in CaO, and depleted in Al_2O_3. In contrast, TiO_2 and Ni contents have remained unaffected. Data sources are available from the authors.

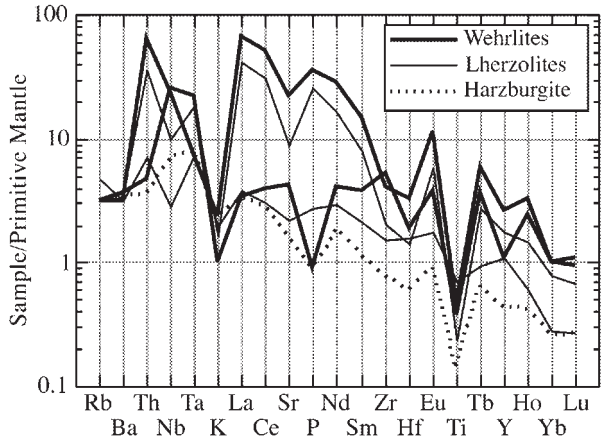

Fig. 4. Trace element abundances of two wehrlites (samples 71001 and 70965), two lherzolites (samples 71008 and 70987), and one harzburgite (sample 76995), normalized to primitive mantle of Sun & McDonough (1989). The wehrlite and lherzolite compositions presented span the measured range of abundances in each rock-type. [See Yaxley *et al.* (1991) for analyses of 71001, 70965, 71008 and 70987, and Table 3 for 76995.]

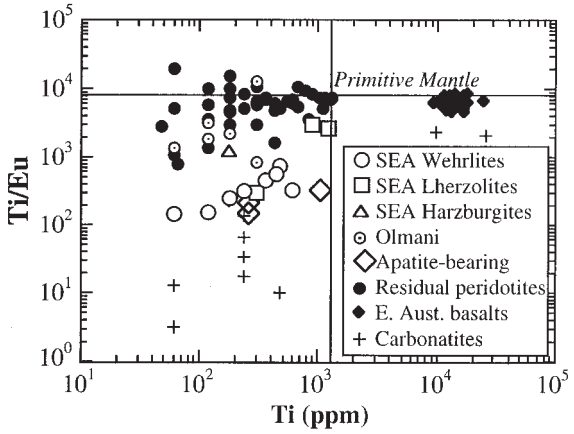

Fig. 5. Plot of whole-rock Ti (ppm) vs Ti/Eu for the wehrlites, lherzolites and harzburgites from SEA, compared with residual peridotites (Frey & Prinz, 1978; Kurat *et al.*, 1980; Nickel & Green, 1984; Preß *et al.*, 1986; Dupuy *et al.*, 1987; O'Reilly & Griffin, 1988; Stolz & Davies, 1988; Song & Frey, 1989), other apatite-bearing xenoliths (O'Reilly & Griffin, 1988; Stolz & Davies, 1988), the carbonatite-metasomatized peridotites from Olmani (Rudnick *et al.*, 1993), carbonatites (Nelson *et al.*, 1988), and basalts from lava field provinces in Eastern Australia (O'Reilly & Zhang, 1995). Primitive mantle from Sun & McDonough (1989).

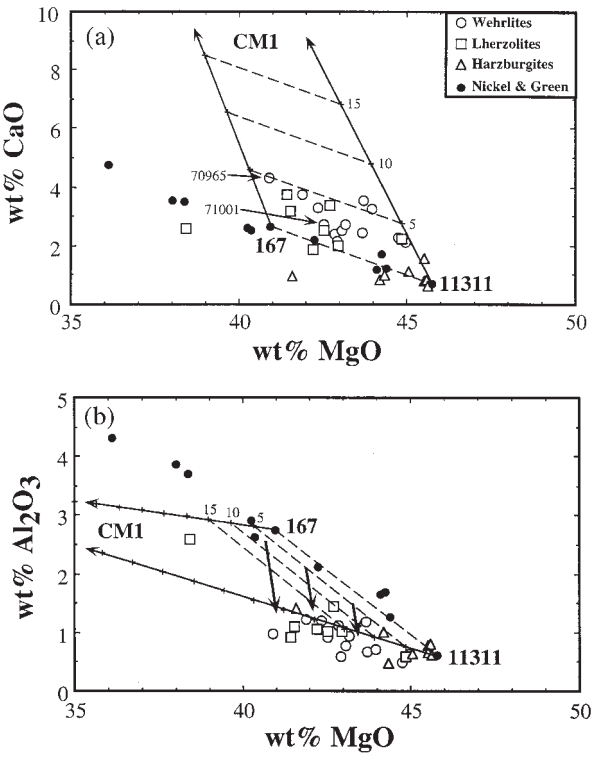

Fig. 6. Plots against wt % MgO of (a) wt % CaO, and (b) wt % Al_2O_3 comparing the whole-rock compositions of the wehrlites, lherzolites and harzburgites with compositions potentially generated by binary mixing between inferred precursor peridotite compositions, which lie along the dashed line between samples 167 (Nickel & Green, 1984) and 11311 (O'Reilly & Griffin, 1988), and the experimental carbonatite composition of Wallace & Green (1988) (CM1). Large arrows are the mixing vectors. Smaller, near-vertical arrows in (b) indicate the inferred direction of change in composition of the lithosphere because of loss during metasomatism of Al_2O_3 in a putative siliceous, aluminous, alkali-rich melt. The dashed lines between, and tick marks on the mixing vectors represent increments of 5% CM1 addition to the range of inferred precursor compositions. This is indicated by the numbers next to the vectors, which refer to CM1 recalculated to be free of the CO_2 component, which is assumed to have escaped during metasomatism. Also shown for reference are compositions of group A1–A5 peridotite xenoliths of Nickel & Green (1984), which illustrate partial melting trends for the lithosphere. (See text for further information.)

and a metasomatic agent with silica activity too low to be in equilibrium with orthopyroxene under lithospheric *P–T* conditions.

Zinngrebe & Foley (1995) attributed the observed replacement of orthopyroxene by clinopyroxene in spinel peridotite xenoliths from West Eifel (Germany) to interactions between deeply derived, low SiO_2 melts and harzburgitic or lherzolitic lithospheric wall-rock. An alternative metasomatic agent, which also has low SiO_2 content, is carbonatite melt (Green & Wallace, 1988). Several experimental studies have shown that dolomitic carbonatite liquids with high *mg*-number* (~85) are stable in equilibrium with lherzolite at pressures greater than ~1·5–2·0 GPa, at near-solidus temperatures (e.g. Wallace & Green, 1988; Thibault *et al.*, 1992; Dalton & Wood, 1993). Should such a melt segregate from its source regions, and ascend, it will cross the reaction enstatite + dolomite = diopside + forsterite + CO_2 at ~1·5–2·0 GPa. Decarbonation reactions between components in the carbonatite and peridotite wall-rock phases (particularly orthopyroxene) will convert refractory harzburgite or lherzolite to wehrlite, with loss of a CO_2-rich fluid (Green & Wallace, 1988; Yaxley *et al.*, 1991; Yaxley & Green, 1996).

Mineral chemical characteristics imply that these samples are more likely to have interacted with carbonatite melt(s), than with deeply derived silicate melt(s). For example, low Al_2O_3 and TiO_2 in relict orthopyroxene and metasomatically introduced clinopyroxene (Fig. 1) are consistent with interactions between precursor peridotite and a metasomatic agent with low Al_2O_3 and TiO_2 (Green & Wallace, 1988). Carbonatites in equilibrium with peridotite are likely to be substantially lower in Al_2O_3 and TiO_2 than asthenospheric silicate melts (Wallace & Green, 1988; Dalton & Wood, 1993). The presence of carbonate-bearing and hydrous phases (e.g. calcitic carbonate, apatite, amphibole and phlogopite) and primary, CO_2-rich fluid inclusions trapped in metasomatic phases, suggests that the metasomatic agent was rich in carbonate and H_2O. If carbonatite melts were responsible for metasomatism of these samples, then the unusually sodic nature of their metasomatically enhanced clinopyroxene indicates that the carbonatite was also sodic (Dalton & Wood, 1993).

The unusual fractionations of trace element ratios not usually significantly affected by petrological processes also support involvement of carbonatites in the metasomatic process. The very low whole-rock Ti/Eu values exhibited by our samples are inconsistent with basaltic metasomatism (Fig. 5). For example, McPherson *et al.* (1996) demonstrated that peridotite wall-rock in the Lherz peridotite massif was significantly modified by interaction with mafic silicate melts now preserved as cross-cutting amphibolite and pyroxenite dykes, but that Ti/Eu in the wall-rock was not significantly fractionated during this process. However, natural carbonatites almost always have Ti/Eu values substantially below that of primitive mantle (range 3–2400, average 574; Nelson *et al.*, 1988) (Fig. 5). Although caution should be exercised when comparing geochemical characteristics of crustal carbonatites with postulated and possibly unrelated metasomatic carbonatites in the lithosphere, experimental determinations of trace element partitioning relationships between inferred mantle carbonatite melt compositions and clinopyroxene or amphibole support the notion that equilibration with carbonatitic melts will lower Ti/Eu in phases in the peridotitic wall-rock (Sweeney *et al.*, 1992, 1995; Klemme *et al.*, 1996). Decoupling of REE and Ti

abundances was a predicted characteristic of carbonatite metasomatized lithosphere (Green & Wallace, 1988).

Elevated Zr/Hf values in mantle xenoliths have been attributed to interaction with metasomatic carbonatites (Dupuy *et al.*, 1992; Rudnick *et al.*, 1993). The Zr/Hf values exhibited by the current suite are also elevated above the primitive mantle value of 36, varying from 34 to 125 (mean 66), consistent with interaction with carbonatite.

The nature of the metasomatic process

The model for carbonatite metasomatism proposed by Green & Wallace (1988) suggests that the associated geochemical perturbation occurs in a predominantly closed system. That is, the metal oxide components of the invasive carbonatite melt are effectively absorbed by the pre-metasomatic lithosphere, with loss of most of a CO_2-rich fluid during decarbonation reactions between peridotite phases (particularly orthopyroxene) and the carbonatite melt. The geochemistry of the affected part of the lithosphere should therefore reflect binary mixing between the metal oxide parts of the carbonatite and the precursor lithosphere. However, Rudnick *et al.* (1993) demonstrated that geochemistry is controlled by open system processes, dependent on partitioning relationships between the reacting, evolving carbonatite, and peridotite phases.

In this section, we model the metasomatic process as simple binary mixing (i.e. closed system metasomatism) between suitable precursor lithospheric compositions and carbonatite melt, to place lower limits on the amounts of carbonatite melt addition necessary to produce the observed chemistry. Samples 167 (Nickel & Green, 1984) and DR11311 (O'Reilly & Griffin, 1988) were chosen as reasonable pre-metasomatic compositions, as they lie within the partial melting trends for the SEA xenolith suite, and because they cover a range of MgO contents similar to that covered by those samples from the current suite whose compositions also lie close to the partial melting trend (i.e. those samples presumed to be least affected by the metasomatism). The experimental sodic dolomitic carbonatite composition of Wallace & Green (1988) (CM1) was chosen to model the metasomatic agent. A number of experimental studies have shown that carbonatite melts in equilibrium with peridotite in the lithosphere are broadly dolomitic (e.g. Wyllie & Huang, 1975; Wallace & Green, 1988; Thibault *et al.*, 1992; Sweeney, 1994; Yaxley & Green, 1996). The outcomes of the modelling described below were not significantly affected by the choice of carbonatite compositions, provided that it was broadly dolomitic.

Figure 6a indicates that the MgO and CaO contents of the wehrlites and lherzolites can be reproduced by simple binary mixing between pre-metasomatic lithosphere with a range of compositions lying along the partial melting trend between samples DR11311 and 167, and CM1. The wehrlite compositions require ~3–6% of the volatile-free metal oxide component of the carbonatite, or ~6–12% carbonatite including the CO_2-rich component. The lherzolites require ~8% or less carbonatite addition (volatile component included). The harzburgites require minimal, or no addition of dolomitic carbonatite, and are presumed to most closely resemble pre-metasomatic compositions in CaO–MgO space. Because of the likely presence of an open system component to the metasomatic process (Rudnick *et al.*, 1993), these estimates of the amount of carbonatite melt addition necessary to drive precursor lithospheric compositions to those of individual, metasomatized xenoliths should be considered lower limits.

In contrast, Al_2O_3 contents of the xenoliths are too low to lie on mixing lines between the assumed protoliths and CM1, or any carbonatite with similar MgO but lower Al_2O_3 contents (Fig. 6b). Assuming that the range of pre-metasomatic lithospheric compositions lay along the peridotite partial melting trend between samples 167 (Nickel & Green, 1984) and DR11311 (O'Reilly & Griffin, 1988), then bulk mixing of 5%, or even 10% CM1 (CO_2 free) would not lower the whole-rock Al_2O_3 content of the affected parts of the lithosphere enough to generate the observed compositions. In fact, addition of 5 or 10% CM1, or any other feasible carbonatite liquid composition, would not perturb whole-rock Al_2O_3 contents significantly from the partial melting trend defined by the group A1–A5 xenoliths of Nickel & Green (1984) (Fig. 6b). Therefore, Al_2O_3 contents of the xenoliths cannot be explained by bulk mixing between refractory precursor lithologies lying on the peridotite partial melting trend, and any feasible liquid composition. This suggests that significant amounts of Al_2O_3 were lost from that part of the lithosphere sampled by these xenoliths during the metasomatic process, and that, consequently, the whole-rock compositions in MgO–Al_2O_3 space have been driven in the direction indicated by the near-vertical arrows in Fig. 6b. Similar calculations also indicate that some SiO_2 may have been lost. Presumably these components partitioned more strongly into the reacting, evolving metasomatic melt than into the newly forming metasomatic phases (mainly clinopyroxene), or the reacting primary phases (orthopyroxene and spinel), consistent with their unusually low Al_2O_3 contents. This may have resulted in formation of a fugitive melt phase, rich in SiO_2 and Al_2O_3, and probably also in alkalis and LILE, but low in CaO and MgO. Unfortunately, testing for loss of alkali components using binary mixing calculations as described above produced equivocal results, because larger scatter in the peridotite partial melting

trends on plots against MgO made estimates of suitable precursor compositions uncertain.

The siliceous, aluminous component must be now largely absent from the xenoliths, to explain their low whole-rock Al_2O_3 and SiO_2. This inferred loss of Al_2O_3 raises the obvious question as to its ultimate fate. Ionov *et al.* (1995, 1997) described alkali-rich feldspar + Ti-oxide-bearing patches and veins in spinel peridotite xenoliths from Hamar-Daban, in the southern Baikal region of Siberia. These feldspar-rich zones are strongly enriched in K, Rb, Ba, and Ti, as well as other incompatible trace and minor elements. Interestingly, many of these elements exhibit strong negative anomalies on the primitive mantle normalized spidergrams for the carbonatite metasomatized xenoliths. Also, Hornig & Wörner (1991) reported siliceous, aluminous and alkali-rich veins (crystallized as leucite + plagioclase + clinopyroxene + nepheline + apatite + Ti-mica + Mg-ilmenite + rare zirconolite at ~0·5 GPa and ~1000°C), in a mantle xenolith hosted by a basanite from the Mt Melbourne Volcanic Field, Antarctica. We speculate that these patches and veins may represent a highly siliceous, aluminous melt phase, enriched in alkalis, Rb, Ba and other LILEs, which has migrated from an inferred zone of carbonatite metasomatism and crystallized the observed phases in veins and fractures in the lithosphere. Thus far, such unusual feldspar-rich patches have not been observed in xenoliths from southeastern Australia. We merely emphasize that the examples described by Hornig & Wörner (1991) and Ionov *et al.*, (1995, 1997) may provide an interesting clue to the fate of the missing Al_2O_3.

CONCLUSIONS

This study and earlier related papers provide strong evidence for the former existence of sodic dolomitic carbonatite melts in the lithosphere beneath southeastern Australia. These melts did not reach the surface, as they reacted with lithospheric phases at 1·5–2·0 GPa (i.e. enstatite + dolomite = forsterite + diopside + CO_2) and metasomatized the lithosphere at this level, producing apatite-bearing spinel wehrlite, lherzolite and harzburgite.

We have demonstrated that much of the clinopyroxene in the lherzolites and wehrlites from our suite was metasomatically introduced by interactions between precursor wall-rock and the dolomitic carbonatites. Mixing calculations suggest that the precursor lithosphere under the localities from which our samples were collected was refractory (~41–46 wt % MgO), probably containing a large proportion of spinel harzburgite. This implies that so-called 'cryptically' metasomatized spinel lherzolite xenoliths (i.e. those exhibiting whole-rock trace element enrichment hosted by clinopyroxene, without additional metasomatic phases such as phlogopite, amphibole or apatite) may have been formed by interaction of relatively small amounts of carbonatite melts with refractory lherzolite or harzburgite, resulting in addition of LILE-enriched clinopyroxene, without other metasomatic phases. Similar conclusions have been reached by Brenan & Watson (1991), Baker & Wyllie (1992) and Rudnick *et al.* (1993). Cryptically metasomatized peridotite xenoliths, as well as xenoliths with clear modal evidence of carbonatite metasomatism, have now been reported from many locations around the world (e.g. Dautria *et al.*, 1992; Hauri *et al.*, 1993; Ionov *et al.*, 1993, 1996; Rudnick *et al.*, 1993; Chazot *et al.*, 1996), indicating that (1) metasomatic enrichment of the lithosphere by carbonatitic melts is a significant world-wide phenomenon, and (2) there have existed in the mantle carbonatites that were never emplaced at crustal levels. The relationship (if any) between these putative mantle carbonatites and carbonatites observed in the Earth's crust may be crucial in understanding the petrogenesis of carbonatites and associated rocks.

ACKNOWLEDGEMENTS

We gratefully acknowledge the technical expertise of Phil Robinson and Wis Jablonski (University of Tasmania), and Frank Brink and David Vowles (Electron Microscopy Unit, The Australian National University). The manuscript benefited from constructive reviews by R. Rudnick, M. Menzies, I. Kjarsgaard and B. Kjarsgaard.

REFERENCES

Baker, M. B. & Wyllie, P. J. (1992). High-pressure apatite solubility in carbonate-rich liquids: implications for mantle metasomatism. *Geochimica et Cosmochimica Acta* **56,** 3409–3422.

Brenan, J. M. & Watson, E. B. (1991). Partitioning of trace elements between carbonate melt and clinopyroxene and olivine at mantle *P–T* conditions. *Geochimica et Cosmochimica Acta* **55,** 2203–2214.

Canil, D. & Scarfe, C. M. (1989). Origin of phlogopite in mantle xenoliths from Kostal Lake, Wells Gray Park, British Columbia. *Journal of Petrology* **30,** 1159–1179.

Chazot, G., Menzies, M. A. & Harte, B. (1996). Determination of partition coefficients between apatite, clinopyroxene, amphibole, and melt in natural spinel lherzolites from Yemen: implications for wet melting of the lithospheric mantle. *Geochimica et Cosmochimica Acta* **60,** 423–437.

Dalton, J. A. & Wood, B. J. (1993). The compositions of primary carbonate melts and their evolution through wallrock reaction in the mantle. *Earth and Planetary Science Letters* **119,** 511–525.

Dautria, J. M., Dupuy, C., Takherist, D. & Dostal, J. (1992). Carbonate metasomatism in the lithospheric mantle: peridotitic xenoliths from a melilititic district of the Sahara basin. *Contributions to Mineralogy and Petrology* **111,** 37–52.

Deines, P. & Gold, D. P. (1973). The isotopic composition of carbonatite and kimberlite carbonates and their bearing on the isotopic composition of deep-seated carbon. *Geochimica et Cosmochimica Acta* **37,** 1709–1733.

Dupuy, C., Dostal, J. & Bodinier, J. L. (1987). Geochemistry of spinel peridotite inclusions in basalts from Sardinia. *Mineralogy Magazine* **51,** 561–568.

Dupuy, C., Liotard, J. M. & Dostal, J. (1992). Zr/Hf fractionation in intraplate basaltic rocks: carbonate metasomatism in the mantle source. *Geochimica et Cosmochimica Acta* **56,** 2417–2424.

Frey, F. A. & Prinz, M. (1978). Ultramafic inclusions from San Carlos, Arizona: petrologic and geochemical data bearing on their petrogenesis. *Earth and Planetary Science Letters* **38,** 129–176.

Frey, F. A., Suen, C. J. & Stockman, H. W. (1985). The Ronda high temperature peridotite: geochemistry and petrogenesis. *Geochimica et Cosmochimica Acta* **49,** 2469–2491.

Green, D. H. & Wallace, M. E. (1988). Mantle metasomatism by ephemeral carbonatite melts. *Nature* **336,** 459–462.

Hauri, E. H., Shimuzu, N., Dieu, J. J. & Hart, S. R. (1993). Evidence for hotspot-related carbonatite metasomatism in the oceanic upper mantle. *Nature* **365,** 221–227.

Hornig, I. & Wörner, G. (1991). Zirconolite-bearing ultra-potassic veins in a mantle-xenolith from Mt. Melbourne Volcanic Field, Victoria Land, Antarctica. *Contributions to Mineralogy and Petrology* **106,** 355–366.

Ionov, D. A., Dupuy, C., O'Reilly, S. Y., Kopylova, M. G. & Genshaft, Y. S. (1993). Carbonated peridotite xenoliths from Spitsbergen: implications for trace element signature of mantle carbonate metasomatism. *Earth and Planetary Science Letters* **119,** 283–297.

Ionov, D. A., O'Reilly, S. Y. & Ashchepkov, I. V. (1995). Feldspar-bearing lherzolite xenoliths in alkali basalts from Hamar-Daban, southern Baikal region, Russia. *Contributions to Mineralogy and Petrology* **122,** 174–190.

Ionov, D. A., O'Reilly, S. Y., Genschaft, Y. S. & Kopylova, M. G. (1996). Carbonate-bearing mantle xenoliths from Spitsbergen: phase relationships, mineral compositions and trace element residence. *Contributions to Mineralogy and Petrology* **125,** 375–392.

Ionov, D. A., Griffin, W. L., Prikhodko, V. S. & O'Reilly, S. Y. (1997). A new type of mantle metasomatism: trace element composition of feldspar-bearing peridotite xenoliths in basalts from southern Siberia. In: *Seventh Annual V. M. Goldschmidt Conference. LPI Contribution 921*. Houston, TX: Lunar and Planetary Institute, p. 102.

Kjarsgaard, B. A. & Hamilton, D. L. (1988). Liquid immiscibility and the origin of alkali-poor carbonatites. *Mineralogy Magazine* **52,** 43–55.

Kjarsgaard, B. A. & Hamilton, D. L. (1989). The genesis of carbonatites by immiscibility. In: Bell, K. (ed.) *Carbonatites: Genesis and Evolution*. London: Unwin Hyman, pp. 388–404.

Klemme, S., van der Laan, S. R., Foley, S. F. & Günther, D. (1995). Experimentally determined trace and minor element partitioning between clinopyroxene and carbonatite melt under upper mantle conditions. *Earth and Planetary Science Letters* **133,** 439–448.

Kurat, G., Palme, H., Spettel, B., Baddenhausen, H., Hofmeister, H., Palme, C. & Wänke, H. (1980). Geochemistry of ultramafic xenoliths from Kapfenstein, Austria: evidence for a variety of upper mantle processes. *Geochimica et Cosmochimica Acta* **44,** 45–60.

Lee, W.-J. & Wyllie, P. J. (1997). Liquid immiscibility between nephelinite and carbonatite from 1·0 to 2·5 GPa compared with mantle melt compositions. *Contributions to Mineralogy and Petrology* **127,** 1–16.

McDonough, W. F. (1990). Constraints on the composition of the continental lithospheric mantle. *Earth and Planetary Science Letters* **101,** 1–18.

McPherson, E., Thirlwall, M. F., Parkinson, I. J., Menzies, M. A., Bodinier, J. L., Woodland, A. & Bussod, G. (1996). Geochemistry of metasomatism adjacent to amphibole-bearing veins in the Lherz peridotite massif. *Chemical Geology* **134,** 135–157.

Nelson, D. R., Chivas, A. R., Chappell, B. W. & McCulloch, M. T. (1988). Geochemical and isotopic systematics in carbonatites and implications for the evolution of ocean-island sources. *Geochimica et Cosmochimica Acta* **52,** 1–17.

Nickel, K. G. & Green, D. H. (1984). The nature of the upper-most mantle beneath Victoria, Australia as deduced from ultramafic xenoliths. In: *Kimberlites II: The Mantle and Crust–Mantle Relationships. Proceedings of the 3rd International Kimberlite Conference*. Amsterdam: Elsevier, pp. 161–178.

O'Reilly, S. Y. & Griffin, W.L. (1988). Mantle metasomatism beneath western Victoria, Australia: I. Metasomatic processes in Cr-diopside lherzolites. *Geochimica et Cosmochimica Acta* **52,** 433–447.

O'Reilly, S. Y. & Zhang, M. (1995). Geochemical characteristics of lava-field basalts from eastern Australia and inferred sources: connections with the subcontinental lithospheric mantle? *Contributions to Mineralogy and Petrology* **121,** 148–170.

O'Reilly, S. Y., Griffin, W. L. & Ryan, C. G. (1991). Residence of trace elements in metasomatized spinel lherzolite xenoliths: a proton-microprobe study. *Contributions to Mineralogy and Petrology* **109,** 98–113.

Preß, S., Witt, G., Seck, H. A., Ionov, D. & Kovalenko, V. I. (1986). Spinel peridotite xenoliths from the Tariat Depression, Mongolia. I: Major element chemistry of a primitive mantle xenolith suite. *Geochimica et Cosmochimica Acta* **50,** 2587–2599.

Rudnick, R. L., McDonough, W. F. & Orpin, A. (1992). Northern Tanzanian peridotite xenoliths: a comparison with Kaapvaal peridotites and inferences on metasomatic interactions. In: Meyer, H. O. A. & Leonardos, O. (eds) *Kimberlites, Related Rocks and Mantle Xenoliths, Vol. 1. Proceedings of the Fifth International Kimberlite Conference*. Brasilia: CPRM, pp. 336–353.

Rudnick, R. L., McDonough, W. F. & Chappell, B. W. (1993). Carbonatite metasomatism in the northern Tanzanian mantle: petrographic and geochemical characteristics. *Earth and Planetary Science Letters* **114,** 463–476.

Song, Y. & Frey, F. A. (1989). Geochemistry of peridotite xenoliths in basalt from Hannuoba, Eastern China: implications for subcontinental mantle heterogeneity. *Geochimica et Cosmochimica Acta* **53,** 97–113.

Stolz, A. J. & Davies, G. R. (1988). Chemical and isotopic evidence from spinel lherzolite xenoliths for episodic metasomatism of the upper mantle beneath southeast Australia. *Journal of Petrology, Special Lithosphere Issue,* 303–330.

Sun, S.-s. & McDonough, W. F. (1989). Chemical and isotopic systematics of oceanic basalts: implications for mantle composition and processes. In: Saunders, A. D. & Norry, M. J. (eds) *Magmatism in the Ocean Basins. Geological Society, London, Special Publication* **42,** 313–345.

Sweeney, R. J. (1994). Carbonatite melt compositions in the Earth's mantle. *Earth and Planetary Science Letters* **128,** 259–270.

Sweeney, R. J., Green, D. H. & Sie, S. H. (1992). Trace and minor element partitioning between garnet and amphibole and carbonatitic melt. *Earth and Planetary Science Letters* **113,** 1–14.

Sweeney, R. J., Falloon, T. J. & Green, D. H. (1994). Experimental constraints on the possible mantle origin of natrocarbonatite. In: Bell, K. & Keller, J. (eds) *Carbonatite Volcanism*. Berlin: Springer Verlag, pp. 189–207.

Sweeney, R. J., Prozesky, V. & Przybylowicz, W. (1995). Selected trace and minor element partitioning between peridotite minerals and carbonatite melts at 18–46 kb pressure. *Geochimica et Cosmochimica Acta* **59,** 3671–3683.

Thibault, Y., Edgar, A. D. & Lloyd, F. E. (1992). Experimental investigation of melts from a carbonated phlogopite lherzolite: implications for metasomatism in the continental lithospheric mantle. *American Mineralogist* **77,** 784–794.

Wallace, M. & Green, D. H. (1988). An experimental determination of primary carbonatite composition. *Nature* **335,** 343–345.

Wyllie, P. J. & Huang, W.-L. (1975). Influence of mantle CO_2 in the generation of carbonatites and kimberlites. *Nature* **257,** 297–299.

Yaxley, G. M. & Green, D. H. (1996). Experimental reconstruction of sodic dolomitic carbonatite melts from metasomatised lithosphere. *Contributions to Mineralogy and Petrology* **124,** 359–364.

Yaxley, G. M., Crawford, A. J. & Green, D. H. (1991). Evidence for carbonatite metasomatism in spinel peridotite xenoliths from western Victoria, Australia. *Earth and Planetary Science Letters* **107,** 305–317.

Yaxley, G. M., Kamenetsky, V., Green, D. H. & Falloon, T. J. (1997). Glasses in mantle xenoliths from western Victoria, Australia, and their relevance to mantle processes. *Earth and Planetary Science Letters* **148,** 433–446.

Zinngrebe, E. & Foley, S. F. (1995). Metasomatism in mantle xenoliths from Gees, West Eifel, Germany: evidence for the genesis of calc-alkaline glasses and metasomatic Ca-enrichment. *Contributions to Mineralogy and Petrology* **122,** 79–96.